EUROPEAN COMMISSION

Community Research

SEVENTH FRAMEWORK PROGRAMME

ARCHER

Collaborative Project (CP)

Co-funded by the European Commission under the Euratom Research and Training Programme on Nuclear Energy within the Seventh Framework Programme

Grant Agreement Number : 269892

Start date : 01/02/2011 Duration : 48 Months

www.archer-project.eu

Archer

Advanced Reactor for Cogeneration of Heat & Electricity-R&D

Destructive PIE reports on EU1 irradiated fuel elements

Authors : LAURIE Mathias (EC-JRC) , Stephane Bremier, Oliver Seeger (JRC-ITU)

ARCHER - Contract Number: 269892
Advanced High-Temperature Reactors for Cogeneration of Heat and Electricity R&D
EC Scientific Officer: Dr. Panagiotis Manolatos

Document title	Destructive PIE reports on EU1 irradiated fuel elements
Author(s)	Mathias Laurie, Stephane Bremier, Oliver Seeger (JRC-ITU)
Number of pages	24
Document type	Deliverable
Work Package	WP 32
Document number	D32.12
Issued by	EC-JRC
Date of completion	16/03/2015
Dissemination level	Confidential, only for members of the consortium (including the Commission Services).

Summary

This report presents the results from the Post Irradiation Examination (PIE) campaign conducted between March 2013 and January 2015 at the JRC-ITU hot cell facilities in the framework of the ARCHER project. The High-Temperature Reactor fuel pebble that was examined is the HFR-EU1/3 pebble irradiated in the HFR-EU1 experiment at the High Flux Reactor in Petten. The gamma spectrometry setup as well as the HFR-EU1 pebbles fission product inventory will be first presented. Prior to the PIE examination, the HFR-EU1/3 underwent a KÃ¼FA test, where the fuel pebble was heated up with a temperature transient up to 1800°C to simulate and be envelope of a depressurization and loss-of forced- circulation accident. In order to proceed to the PIE analyses, three samples were obtained by carrotage through the diameter of the KÃ¼FA tested sphere, followed by axial cutting into segments. The set of techniques (mainly optical microscopy, SEM, SIMS and acoustic microscopy) used to perform the destructive PIEs on the different HFR-EU1/3 samples as much as the different results achieved will be presented and discussed.

Approval

Date	By
16/03/2015	Mathias LAURIE
16/03/2015	Mathias LAURIE
16/03/2015	Steven KNOL

Distribution list

Name	Organisation	Comments
P. Manolatos	EC DG RTD	Through the EC participant portal
All beneficiaries	ARCHER	Through the private online workspace

EUROPEAN COMMISSION
Directorate General Joint Research Centre
Institute for Energy and Transport – Unit F.04

16 March 2015
PUBSY JRC 94676

JRC TECHNICAL REPORT

Destructive PIE reports on EU1 irradiated fuel elements (Deliverable D 32.12)

rev. 1

Deliverable D32.12 for the FP7 ARCHER Project

Contract Number: 269892

Mathias Laurie, Stephane Bremier, Oliver Seeger (JRC),

	For the Authors	Reviewed by	Verified by	Approved by Unit Head
Name	M. Laurie	S. Bremier		V. Rondinella
Date	16/3/2015	16/3/2015		16/3/2015
Signature		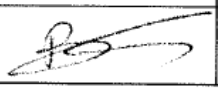		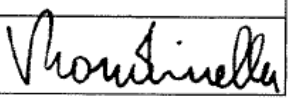

Table of contents

1. Introduction

The HFR –EU1 experiment was designed for testing spherical High Temperature Reactor (HTR) fuel pebbles for their potential for high temperature performance and very high burn up. These pebbles contain fissile material in the form of TRISO coated particles which are composed of UO_2 fuel kernels with successive isotropic layers of porous carbon, dense carbon, dense silicon carbide and dense carbon. Some 10,000 of these particles are embedded in a graphite a sphere of 6 cm diameter.

This report presents results in the framework of the ARCHER project concerning the Post Irradiation Examination (PIE) of the HFR-EU1/3 pebble. The three samples originating from the carroting from the pebble were studied by different PIE means (mainly optical microscopy, SEM, SIMS and acoustic microscopy) and the achieved results are discussed in the present report.

2. Irradiation conditions

The HFR-EU1 irradiation experiment was performed during two European Framework Programs. The irradiation itself has been performed within RAPHAEL (ReActor for Process Heat And Electricity), a 4-year FP6 Integrated Project on Very High Temperature Reactors. The current nondestructive examination, performed by JRC-ITU, belongs to the FP7 project ARCHER (Advanced High-Temperature Reactor for Co-generation of Heat and Electricity R&D) [1].

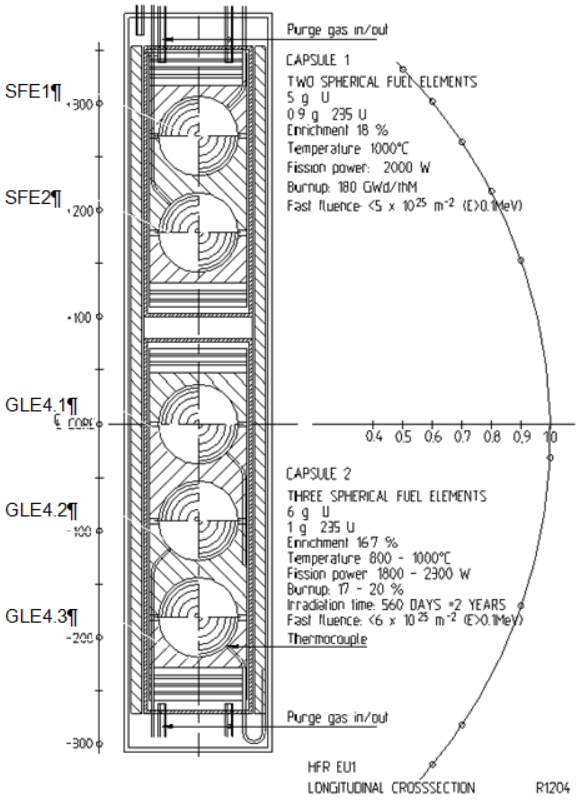

Coated Particle	INET	AVR
Particle batch	V000802	HT-384-393
Kernel composition	UO_2	UO_2
Kernel diameter [µm]	490.3	502
Enrichment [U-235 wt.%]	17.08	16.76
Thickness of coatings [µm]:		
→ buffer	97.7	92
→ inner PyC	42.0	40
→ SiC	37.8	35
→ outer PyC	40.8	40
Particle diameter [µm]	926.9	916
Pebble		
Heavy metal loading [g/pebble]	5.02	6.0
U-235 content [g/pebble]	0.858	1.00 ± 1 %
Number of coated particles per pebble	8500	9560
Volume packing fraction [%]	5.0	6.2
Defective SiC layers [U/U_{tot}]	2.3×10^{-7}	7.8×10^{-6}
Matrix graphite grade	A3-3	A3-3
Matrix density [kg/m³]	1760	1750
Temperature at final heat treatment [°C]	N/A	1900

Figure 1 Conceptual sketch of HFR-EU1 and characteristics data of the pebbles

The HFR-EU1 experiment included 5 pebbles of 60 mm diameter respectively named HFREU1-1 to HFREU1- 5. HFR-EU1/1 and /2 are originating from INET, while pebbles HFR-EU1/3 to HFR-EU1/5 are German pebbles type GLE-4 (reload 21/2). The pebbles were embedded in a graphite matrix in the form of half-shells. The characteristics of the pebbles embedded in a graphite matrix in the form of half-shells are given in Figure 1.

The irradiation initially planned to be performed for 22-24 cycles in core position H2 (Figure 2) started on 30 September 2006, i.e. after the conversion of the HFR core to low-enriched uranium (LEU). As it turned out that the heat developed by the fuel in H2 was about 20-30% lower than calculated, the experiment was moved to position H4 and lately to position F2 until the end of irradiation.

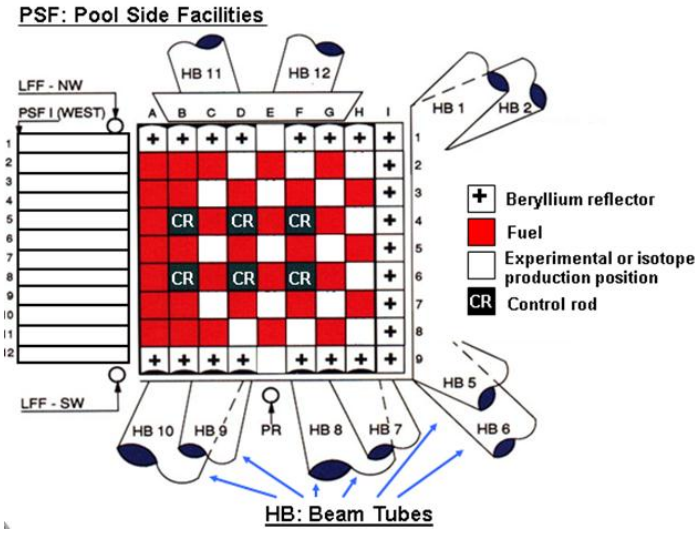

Figure 2: HFR standard core configuration

The irradiation test was performed in two campaigns, from 29 September 2006 to 24 February 2008 (12 reactor cycles of 28 days each) and continuing from 19 October 2009 to 19 February 2010 (4 reactor cycles), for a total of 445 efpd. The fluences provided cycle by cycle are given in Table 1.

Cycle	Core Position	efpd	Φ_1 [1]	Φ_2 [1]	Φ_3 [1]	Φ_4 [1]	thermal fluence	fast fluence (E> 0.1 MeV)
		[days]	Cycle averaged [10^{18} $m^{-2}s^{-1}$]				[10^{24} m^{-2}]	
2006-08	H2	24.2	0.409	0.612	0.602	0.697	1.46	1.63
2006-09	H2	26.9	0.412	0.615	0.603	0.691	1.60	1.82
2006-10	H2	28.6	0.443	0.645	0.632	0.730	1.80	3.05
2007-01	H4	27.9	0.695	0.927	0.873	0.866	2.09	3.05
2007-02	H4	28.9	0.720	0.974	0.915	0.878	2.19	3.30
2007-03	H4	27.9	0.710	0.963	0.907	0.878	2.11	3.14
2007-07	F2	27.5	0.778	1.078	1.049	1.106	2.62	3.39
2007-08	F2	28.7	0.790	1.097	1.069	1.139	2.83	3.61
2007-09	F2	28.0	0.786	1.089	1.060	1.118	2.70	3.49
2007-10	F2	27.8	0.762	1.054	1.024	1.072	2.58	3.36
2008-01	F2	27.8	0.746	1.035	1.010	1.066	2.56	3.29
2008-02	F2	28.8	0.795	1.103	1.077	1.149	2.85	3.63
2009-08	F2	24.8	0.770	1.088	1.060	1.101	2.36	3.06
2009-09	F2	31.4	0.778	1.099	1.070	1.111	3.011	3.91
2009-10	F2	24.3	0.766	1.082	1.054	1.087	2.284	2.98
2010-01	F2	31.7	0.757	1.070	1.043	1.086	2.971	3.84
total		444.88					38.02	49.51

Table 1: Measured fluences for HFR-EU1 cycle per cycle

The calculated average burn-up per pebble is given in Table 2 [1].

Spherical Fuel Element	Origin	Burnup (% FIMA) (estimated)
HFR-EU1/5	Germany (GLE4/AVR)	13.47
HFR-EU1/4		14.33
HFR-EU1/3		13.90
HFR-EU1/2	China (INET)	11.65
HFR-EU1/1		9.28

Table 2: Estimated Burn-up for each pebble

3. JRC-ITU gamma spectrometry setup

The fission product inventory of the fuel elements is to be determined by gamma spectrometry. For this purpose, the pebble to be measured is placed inside the Hot Cell in front of a conical collimator installed in an opening in the cell wall. On the other side of the opening, in the operation area, a high-purity germanium detector is positioned with high energy resolution.

The measurement system was performed with a newly purchased HPGe detector (30% efficiency dedicated to low energy measurements with a carbon epoxy entrance window) liquid nitrogen cooled. The acquisition was performed by the use of a DSA 1000 and the spectra were acquired with Interwinner and analyzed by Genie 2000.

3.1 Cell 101 setup

The collimation system is attached physically to the Cell 101 in the Hot Cells. Two systems are available according to the radioactive sources (either fuel pins or pebbles) to be measured. When dealing with the HTR pebbles, a dedicated pinhole system composed of several Denal pieces housed in a tailored made tube is used. The collimator penetrates through the concrete wall of about 1 m thickness and targets the pebble placed in a tin box that allows a reproducible positioning of the pebble. The tin box is mounted on a rotating table to take into account the 3D particles inhomogeneity within the pebble. A laser system assesses the positioning of the pinhole collimator with respect to the tin box (used as pebble support). An overview of the system is provided in Figure 3.

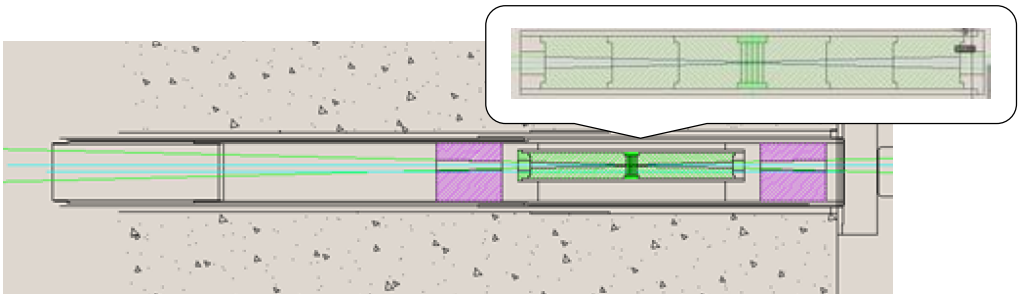

Figure 3: Pinhole collimator system

The collimation function was performed by using a ^{137}Cs source quasi punctual (i.e. 2.7 mm length) with a sufficient activity to allow a reasonable counting time (i.e. 3.7 10^9 Bq in April 1991). The HPGe detector being ISOCS compatible, the collimation function and the efficiency achieved with the ^{137}Cs source were assessed by specific MCNP type calculations (Figure 4). The expected pinhole size of 0.8 mm was found too large to fit with the performed measurements. We deduced from the MCNP assessment a slight mechanical displacement of the Denal blocks encased in the stainless steel tube that reduces the pinhole to about 0.65 mm.

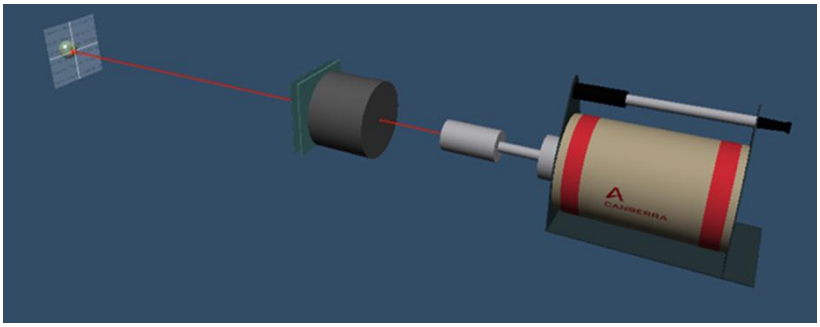

Figure 4: ISOCS geometrical layout for the gamma measurement

An example of the spectra acquired during the measuring campaign is provided in Figure 5.

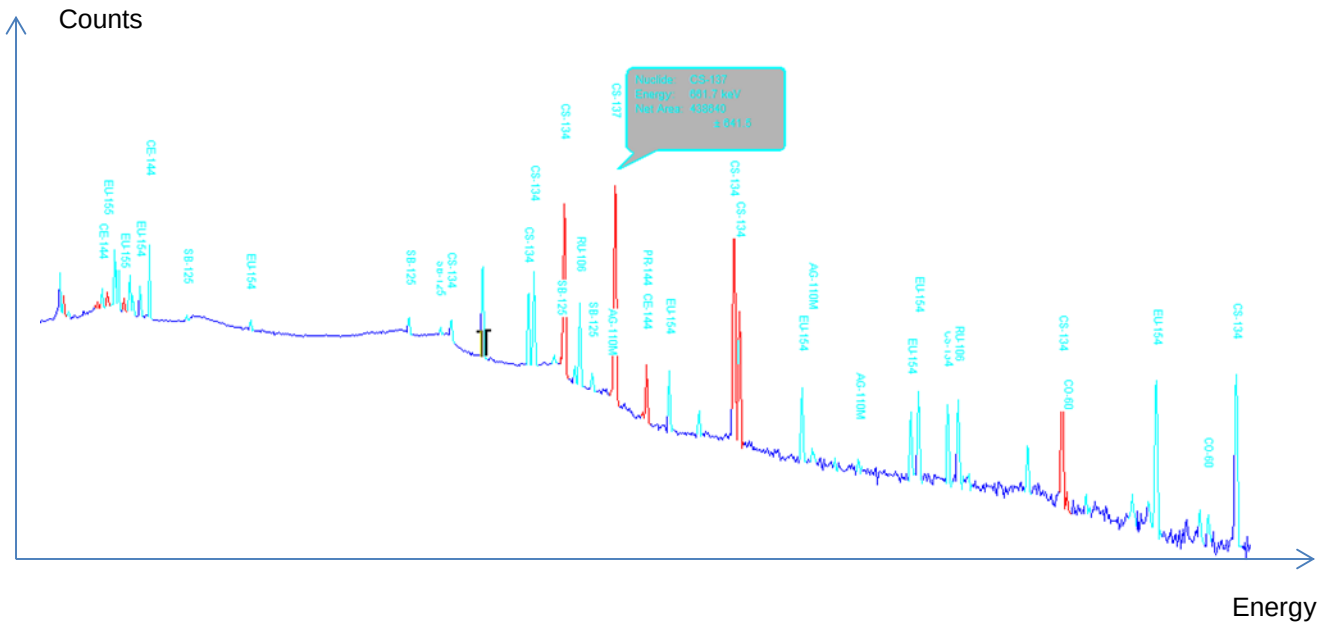

Figure 5: Example of HFR-EU1 spectrum acquired using the JRC-ITU setup

3.2 Efficiency determination

The efficiency curve deduced from the ISOCS calculations and extra measurement is provided in Figure 6. The final version of this curve and the overall calibration process will be presented extensively in Oliver Seeger´s PhD thesis (to be released at the beginning of 2015).

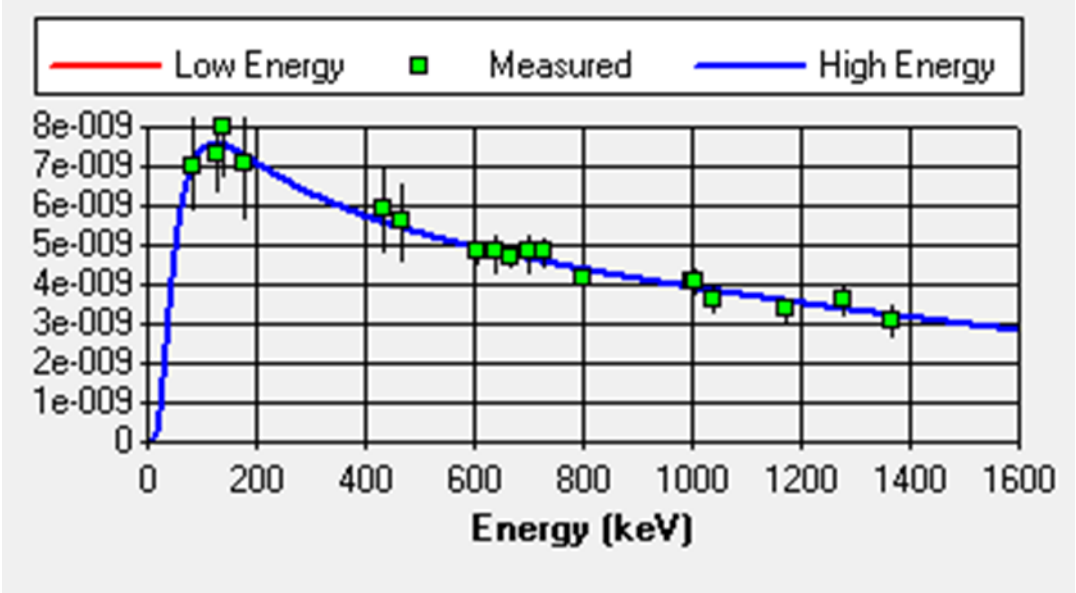

Figure 6: Efficiency curve calculated for the HFR-EU1 pebbles

The following tables are providing the best estimate preliminary activities (at the End Of Irradiation) concerning the HFR-EU1 pebbles HFR-EU1/3 and HFR-EU1/4.

Pebble 3

03/02/2014	Activity (Bq) EOI	Uncertainty
Ru 106	2.75E+11	1.66E+10
Ag 110 m	1.43E+09	1.58E+08
Sb 125	4.54E+09	3.02E+08
Cs 134	1.25E+11	4.38E+09
Cs 137	9.53E+10	2.75E+09
Ce 144	7.31E+11	8.10E+10
Eu 154	3.64E+09	2.72E+08
Eu 155	2.64E+09	2.35E+08
Am 241	5.33E+08	2.20E+08

12/03/2013	Activity (Bq) EOI	Uncertainty
Ru 106	2.74E+11	3.05E+10
Ag 110 m	1.41E+09	2.25E+08
Sb 125	4.50E+09	3.77E+08
Cs 134	1.21E+11	5.45E+09
Cs 137	9.48E+10	2.79E+09
Ce 144	7.21E+11	1.77E+11
Eu 154	3.62E+09	2.91E+08
Eu 155	2.77E+09	2.63E+08
Am 241	4.78E+08	2.20E+08

Pebble 4

12/02/2014	Activity (Bq) EOI	Uncertainty
Ru 106	2.76E+11	1.67E+10
Ag 110 m	1.12E+09	1.38E+08
Sb 125	4.44E+09	2.96E+08
Cs 134	1.26E+11	4.39E+09
Cs 137	9.44E+10	2.73E+09
Ce 144	7.32E+11	8.11E+10
Eu 154	3.66E+09	2.74E+08
Eu 155	2.68E+09	2.37E+08
Am 241	4.81E+08	1.99E+08

Following the Burn-up determination technique described in ref [2], the first burn-up preliminary results provided in Table 3 concerning the HFR-EU1/3 and HFR-EU1/4 pebbles are in reasonable accordance with the calculated one [3].

Spherical Fuel Element	Origin	Burnup (% FIMA) (estimated)	Calculated B.U. % FIMA
HFR-EU1/5	Germany (GLE4/AVR)	13.47	
HFR-EU1/4		14.33	14,58
HFR-EU1/3		13.90	14,64 - 14,72

Table 3: Burn-up estimation

4. HFR-EU1/3 KüFA test

The HFR-EU1/3 KüFA test started on 7 May and ended on 13 June 2014. The initial temperature schedule was:

- heated to 1050°C (similar to irradiation temperature) and held for 30 min.
- heated to 1250°C with the same rate and held at that temperature for 90 min.

After the aforementioned mini temperature plateau, the test entered the accident phase of the experiment for the pebble:

- heating to 1600°C with a 47°C/h ramp and holding at this temperature for 300 h.
- Subsequently, heating to 1800°C continuously (at the same rate) and holding for 200 h.
- The final cool down to 30°C took place at a rate of 75°C/h.

The heating sequence needed to be modified due to unforeseen events, making the total duration of this heating test approximately 744 h instead of the originally planned 564 h

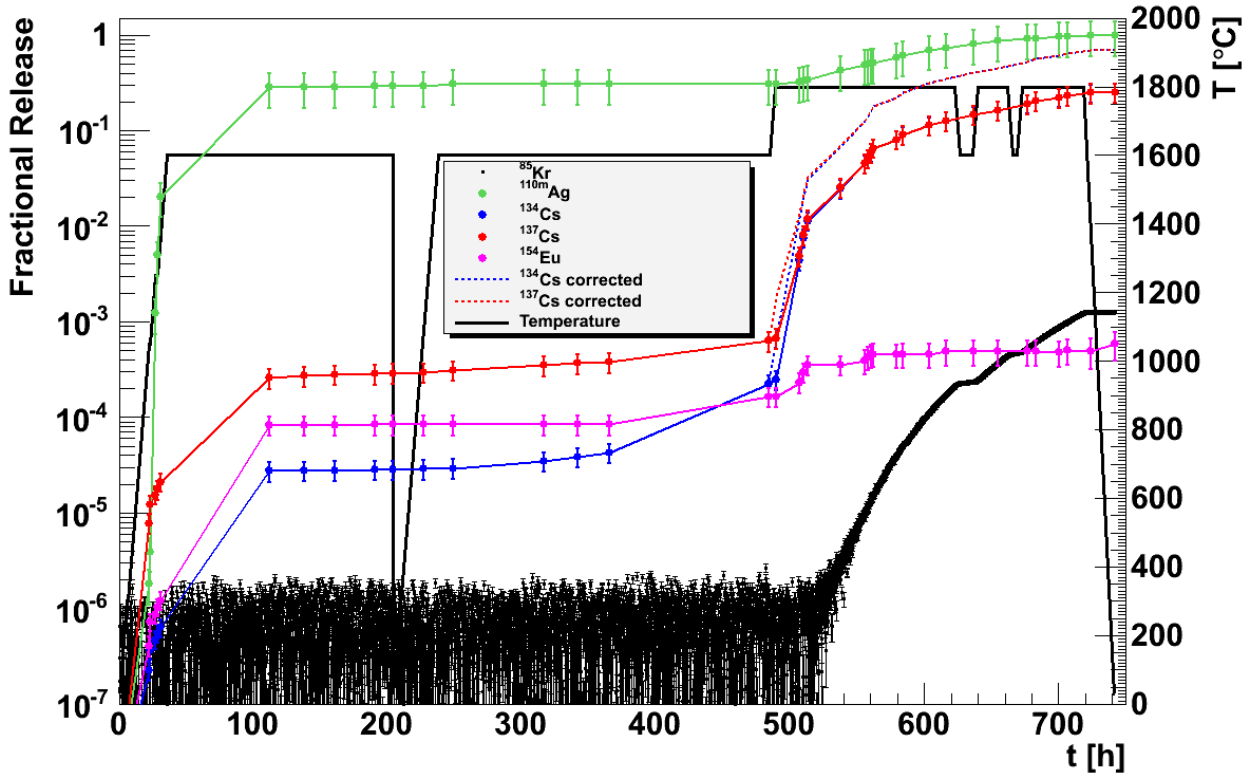

Figure 7: HFR-EU1/3 KüFA test pebble

HFR-EU1/3 retained all fission products except Ag-110m well up to the beginning of the 1800°C accident phase. Slightly more than 10-4 of the Eu-154 and slightly less than 3 × 10-4 of the Cs-134 inventory were released up to this point of the experiment while Kr-85 could not be seen at all. At 1450°C on the heating ramp to 1600°C already 2 × 10-2 of the Ag-110m inventory was released even before the reference accident temperature was reached. Throughout the 1800°C phase of the HFR-EU1/3 KüFA test, the entire Ag-110m inventory of the pebble was released and also the Cs release increased to about 70 %, significantly exceeding all previous heating tests carried out at JRC-ITU. This was expected to happen due to the high burn-up (14 % FIMA) of HFR-EU1/3. Furthermore, a total fraction of (6 ± 2) × 10-4 Eu-154 was released and, again after 40 - 50 h into the 1800°C accident phase, the release of Kr-85 became significant and amounted to (1.263 ± 0.006) × 10-3 at the end of the campaign, corresponding to 12.1 coated particle inventories.

5. **Sample preparation**

A cylindrical carrot was extracted from the spherical fuel element by drilling through an arbitrary diameter of the pebble with a hollow drill, as shown in Figure1. The outer diameter of the drill was 20 mm, the inner diameter ≈ 18.5 mm. The length of the carrot was initially identical to the diameter of the pebble (60 mm).

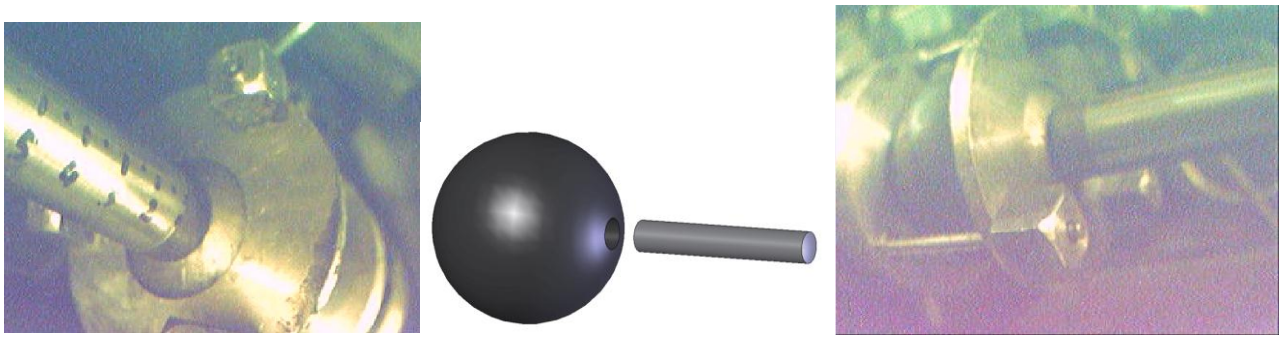

Figure 8: Sketch of drilled fuel element with extracted carrot and pictures of the drilling process

The carrot was cut in five positions placed at distances ≈ 6.0 mm, ≈ 12 mm, ≈ 18 mm, ≈ 27 mm and ≈ 33 mm. The faces to be analyzed from the three samples extracted (i.e. 1076 outside radius, 1075 medium radius and 1074 inner pebble) are presented in bold in the cutting plan shown in Figure 9.

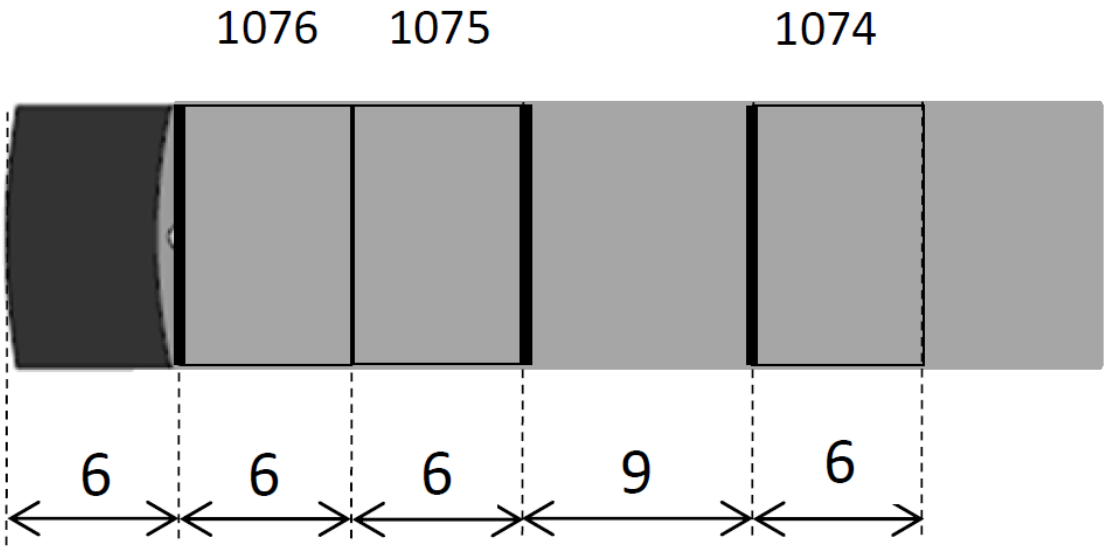

Figure 9: HFR-EU1/3 cutting plan

The obtained cylindrical samples were labelled 1074, 1075, 1076 and embedded in tailored shape sample holders.

The fuel samples were embedded in epoxy resin in cylindrical aluminium holders in which grooves had been machined in the upper and lower parts to facilitate handling by manipulators. To ensure that the resin completely impregnated the sample, embedding was carried out under vacuum. This was carried out in a small chamber which was evacuated using a miniature pump.

Standard metallographic practice was employed. Fine grinding of the sample was carried out using 75 micron diamond paper and water as a lubricant. Grinding was followed by polishing with a series of water-based diamond powder suspensions of increasing fineness. For grinding and polishing, the sample was mounted in a compartment and held against the rotating disc of the grinding/polishing machine. Prior to examination in the optical microscope and between each preparation step, the sample was washed.

6. **Optical microscopy and SEM examination of sample 1074**

After complete hardening of the resin, the samples were polished to a surface finish of 1 µm and thoroughly cleaned with water.

The fuel samples were examined using a Leica Telatom-3 light optical microscope. The microscope is connected to the sample preparation cell by a conveyor belt. The first step in the examination of each sample was the production of an optical macrograph showing the entire sample

The overview photo (Figure 10) of the sample 1074 extracted from the fuel pebble centre exhibits more than 10 particles with a visible UO2 kernel still attached. The preparation procedure involving cutting, handling, grinding and polishing process may induce UO2 kernel falling out (leaving the buffer and TRISO-layers in

place). Generally particles fall out spontaneously as soon as more than half of the particle is removed by grinding/polishing and the missing UO_2 kernel is detected as a large black spot (5 to be seen in Figure 10). The sample 1074 was conveyed to the SEM for further examinations

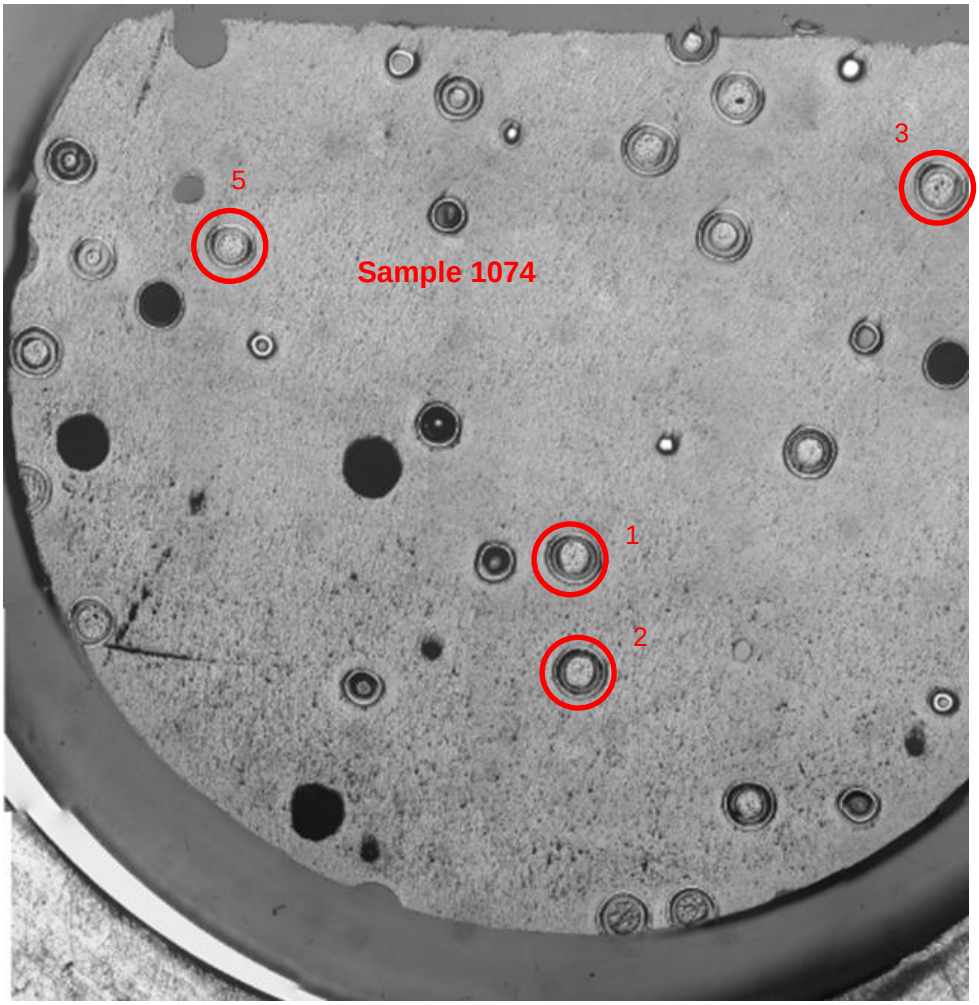

Figure 10: Optical microscopy view of the cross-sectional plane of the sample 1074

The apparatus used for the ceramography of the carrotage sample is a scanning electron microscope (Jeol JSM-6400) mounted in a lead-shielded glove box. The device is equipped with a SAMx (IDFix software) energy dispersive X-ray spectroscopy (EDX) system for elemental analysis that was not operational at the time of the analysis. Table 1 summarizes the main operating parameters of the SEM apparatus

Electron beam			
Accelerating voltage:	30 kV	Number of channels:	2048
Electron beam current:	740 pA	Energy per channel:	10 eV
Detector			
Crystal material:	Si	Resolution (FWHM):	139 eV
Active area:	10 mm^2	Dead layer thickness:	0.1 µm
Crystal thickness:			
Geometry			
Rotation angle:	65°	Detection angle:	22°

Table 1: Main operating parameters of the Scanning Electron Microscope

The relative location of images at higher magnification with the SEM is indicated by circles in Fig. 10.

An overview of complete coated particles is shown in Figures 11 to 14 at an instrument magnification of 100× on the left side. The boundaries between the kernel and all coating layers are well-defined, with gaps between the kernel and the buffer layer. Some delamination phenomena (between the low and high density PyC) can be seen in Fig 12. On these three particles small cracks on the SiC layer could be detected that are enough to lead to a complete release of highly volatile fission products (e.g. Cs that achieve an overall release of around 70% at the end of the KüFA process for the whole pebble). In some cases, as depicted in Fig 12, the crack in the SiC is relatively large and may have been induced by mechanical constraints that operated on the coated particle. Considering the position of the kernel in the sample, the drilling process (that is generating some cracks on the particles close to the drilling area) is not to be considered as a reasonable cause. The small cracks in the SiC layer were discovered on most of the coated particles considered for examination. The delamination phenomena and some clear pathway form the buffer layer to the SiC layer as depicted in the Fig 14 may indicate that the SiC was in contact with carbon monoxide or Fission Products chemical attack that promoted a crack formation.
Considering that the EDX was not operational, generic information concerning the FP deposits will not be provided.

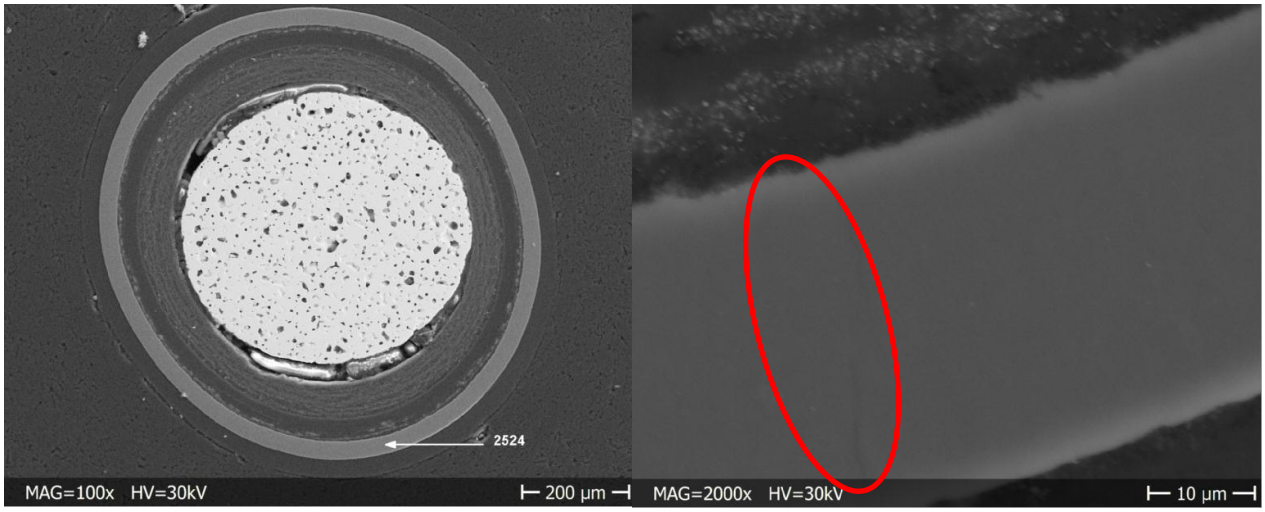

Figure 11: SEM micrographs sample 1074 (kernel 1 + detail 2524 SiC crack)

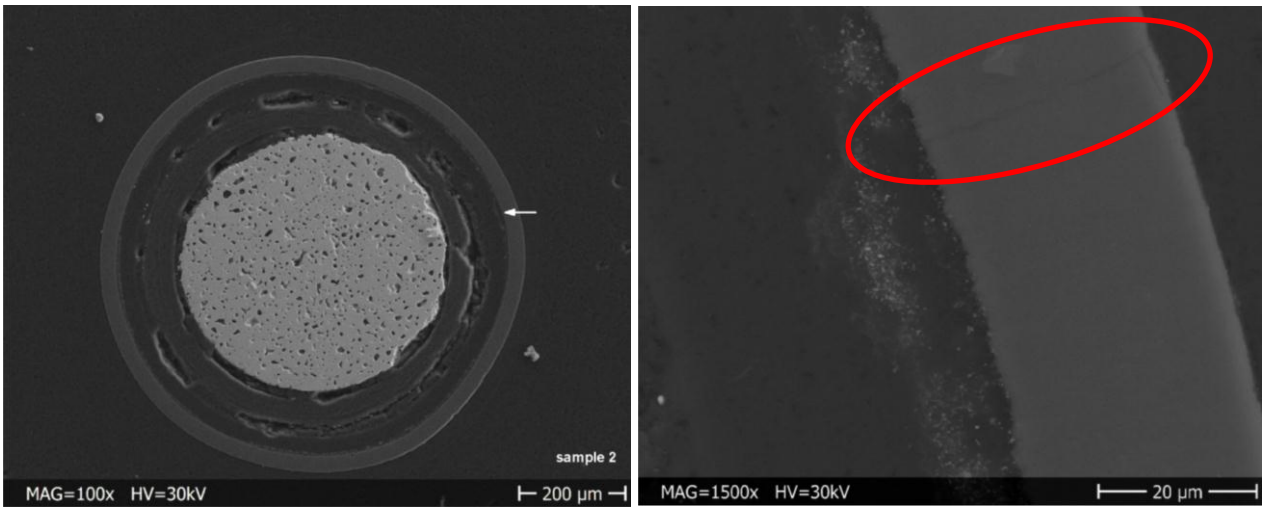

Figure 12: SEM micrographs sample 1074 (kernel 2 + detail on SiC crack)

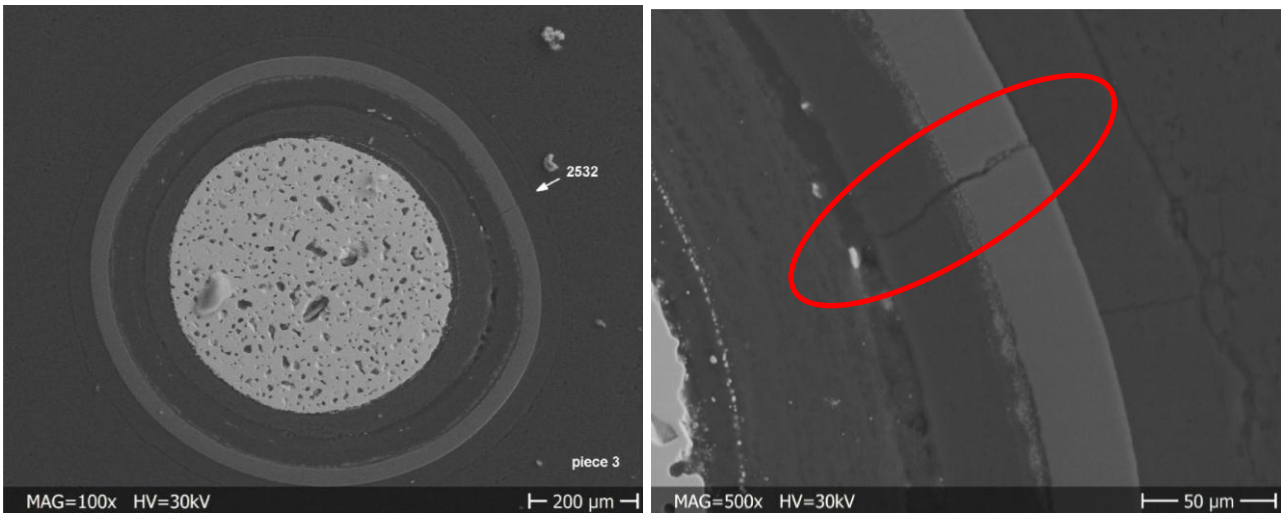

Figure 13: SEM micrographs sample 1074 (kernel 3 + detail on SiC crack)

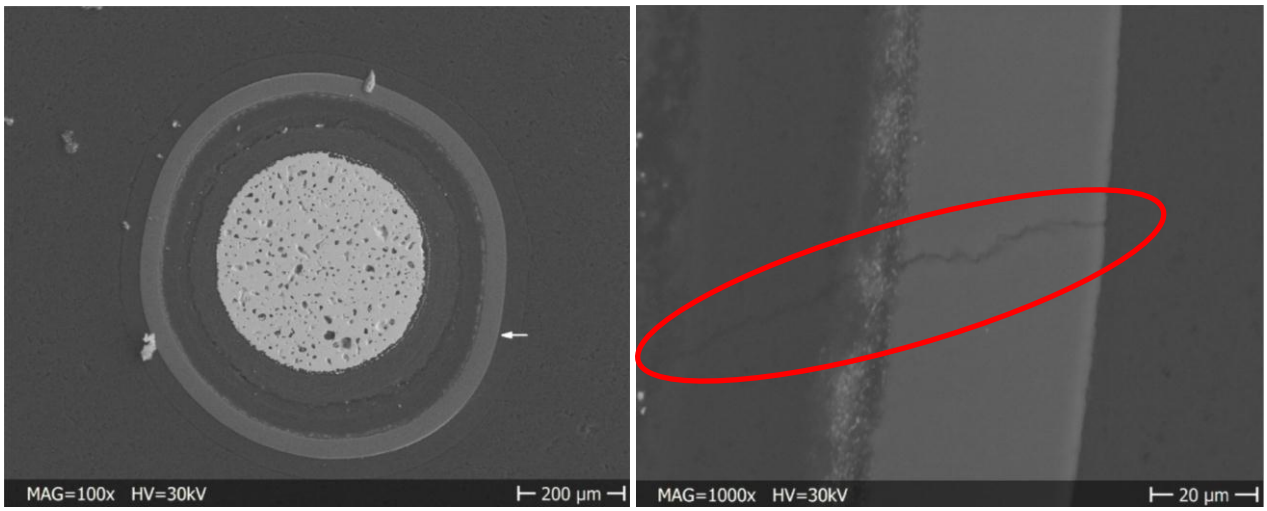

Figure 14: SEM micrographs sample 1074 (kernel 5 + detail on SiC crack)

7. Optical microscopy and SIMS examination of sample 1075

Sample 1075 was selected for subsequent examination with the SIMS. Considering the quite tight planning before the closure of the ARCHER project only the analysis of the coted particle inside the red circle will be taken into account.

Figure 15: View of the cross-sectional plane of the sample 1075

The SIMS analysis was carried using a CAMECA IMS-6F, double-focusing sector field instrument that had been specially shielded and modified for the analysis of irradiated nuclear fuel. A description of the installation can be found in ref. [4]. A $\left(^{16}O\right)_2^+$ primary ion beam was employed. Depending on the objectives of the analysis different instrument settings were employed. The primary and secondary acceleration voltages were +10 and +5 kV, respectively and a beam current of 100 pA was employed. Ion maps were recorded along the particles radius at intervals of 75 µm. At each location the primary beam was scanned over an area measuring 80 x 80 µm. The integration time for an individual isotope ranged from 6.13s to 20.05s, the ion maps were constructed by superimposing 25 raster scans for a total acquisition time per isotope between 153.25 to 501.25 s. The secondary ion signals were all collected with an electron multiplier detector. Table 2 lists the measurement conditions for each species analyzed.

Species	Mass (amu)	Mass field	Detector	Waiting time (s)	Counting time (s)
12C	12.000	19	EM	1.67	6.13
28Si	27.977	29	EM	1.67	6.13
84Kr	83.911	50	EM	1.67	20.05
90Sr	90.000	51	EM	1.67	12.25
102Ru	101.904	55	EM	1.67	7.80
106Pd	105.903	56	EM	1.67	12.25
110Ag	110.000	57	EM	1.67	12.25
137Cs	137.000	63	EM	1.67	12.25
142Nd	141.908	64	EM	1.67	12.25
155Eu	155.000	67	EM	1.67	12.25
238U16O2	270.041	88	EM	1.67	6.13

Table 2: Conditions used for secondary ion mass spectrometry analysis of the particles

The false color ion maps presented in Fig 16 to 19 provide qualitative information about the distribution of the species analysed. The color code (thermal lut) selected for the intensity count rate is the same for all elements at all positions. Attention is drawn to the fact that the reported ion count rates and isotope ratios have not been corrected for mass interference by the isotope hydride [5] and that direct comparison between the ion intensities of a given species measured in different phases (i.e. UO2 and PyC or UO2 and SiC) should be avoided. Owing to limited time to perform measurements, special care was not taken to investigate in detail mass interferences. Some more extensive measurements and analysis will be made available in the months to come and will promote further investigations.

Grain crystallographic orientation affects the local ionisation yields of species; the $^{238}U^{16}O^{2}$ ion map presented in Fig 16 is a good example where UO2 grains exhibit a range of ion count rates

Fig 16 illustrates the typical distribution determined by this analysis: Kr is mostly observed in pores; Cs is hardly to be seen in the fuel matrix which seems in line with the fact that most of the Cs was released during the KüFA test. The top right corners of the Cs and Kr ion maps pinpoint an increase in the count rate outside of the UO2 fuel which is consistent with their volatile nature.
The local gradients observed in the Nd ion map of the Fig 16 are related to the grain crystallographic orientation effect on the yields, as observed also for UO2 (this effect sounds plausible also for Eu and Ag, being less obvious for Sr and Pd).
Inside the fuel, the round metallic precipitates (observed in the optical image) are containing Ru and Ag but no Pd, nor Sr.

The optical image in Fig 17 shows a dark 'gap' between the fuel and the first porous PyC layer. This could probably be some shadowing effects of the camera on areas slightly below the surface of the fuel (potentially originating from the polishing process). The effective size of the gap between the fuel and the first PyC layer is to be assessed in the middle of the C map (red arrow). The Si map depicts only local pollution originating either from the polishing steps or from the polishing liquids (that also contain Si traces).

Fig 17 is consistent with volatile FP release, as indicated firstly by a higher count rate of Kr and Cs in the PyC area than in the fuel, and, secondly, by a decreasing gradient for Sr, Pd, Ag, Eu from the interface

towards the PyC layer (e.g. the Sr main gradient being between 10 to 20µm). High intensity spots (precipitates) containing Sr, Pd and Eu but no Ag are observed at the fuel/PyC interface.

Some local increasing intensity observed for Sr, Pd, Ag, Eu, but also UO2 and Nd (green arrows in Fig 17) may have been the result of an accumulation of material originating from the polishing trapped in small pores.

As already discussed for Fig 17, the optical image in Fig 18 artificially expand the size of the gap between the two PyC layers. The edges are visible in the middle of the C and Cs map (two red arrows indicating the size of the gap) with local increases of the intensity due to edge effects.
The vertical band on the left side of the Cs map is due to an artefact (i.e most probably a glitch during the acquisition process).
As already mentioned for Fig 17, Fig 18 exhibits some local high count rate for Pd, Ag, Eu with Nd and UO_2 that should be related to polishing pollution.
Areas exhibiting precipitations of both Ag and Pd are visible in Fig 19 at the vicinity of the SiC interface. Pd and Ag maps confirm the presence of Pd/Ag rich area close to the interface between PyC and SiC. The fact of having for most of the elements a very significant decrease in count rate between the inner part of the coated particle and the outside confirms the successful barrier effect of the SiC layer.

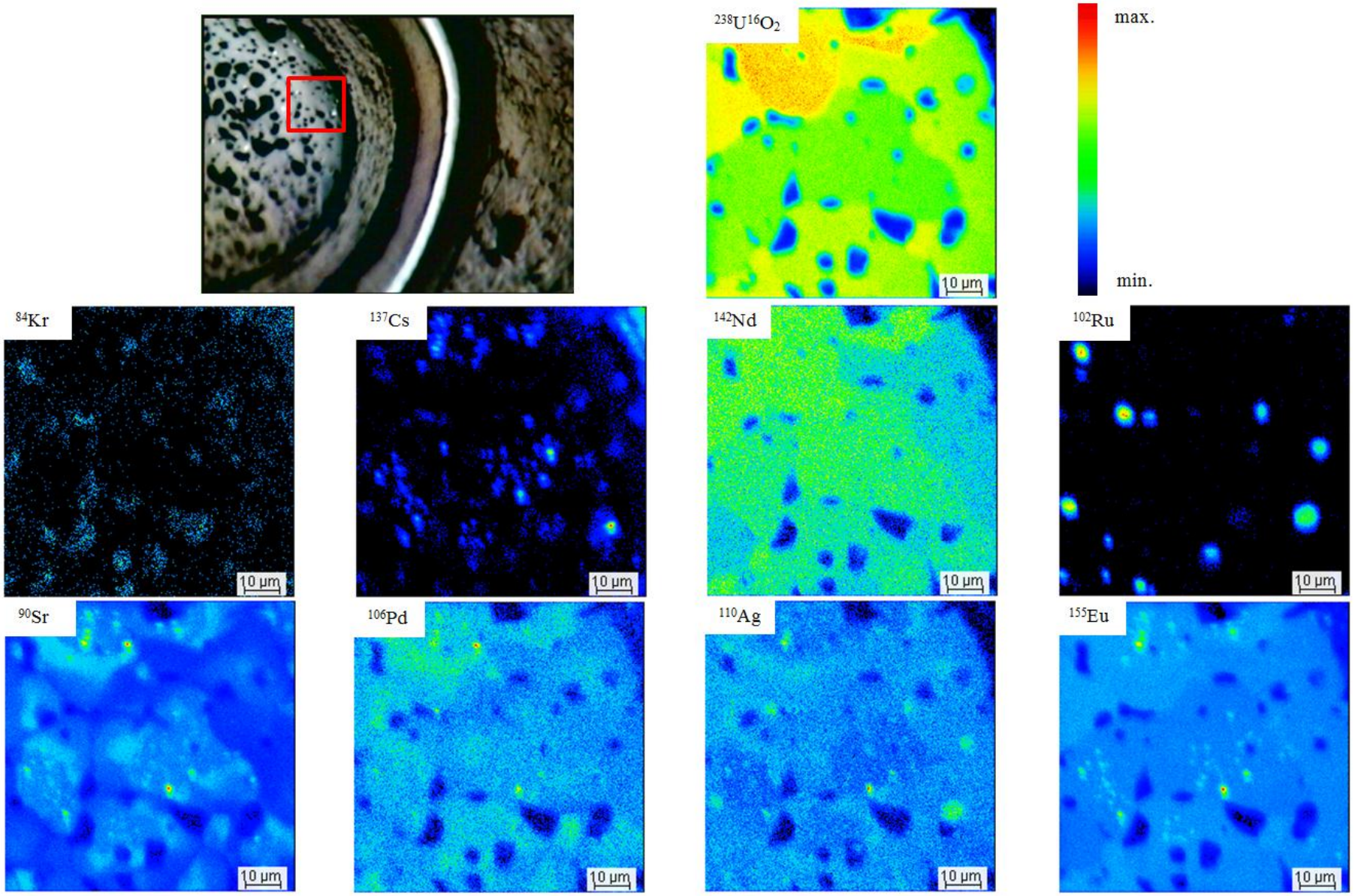

Fig 16: Optical image and ion maps showing the distribution of ^{28}Si, ^{12}C, ^{84}Kr, ^{137}Cs, ^{142}Nd, $^{238}U^{16}O^{2}$, ^{90}Sr, ^{106}Pd, ^{110}Ag and ^{155}Eu in the fuel aera. The red square on the optical image shows the analysed area.

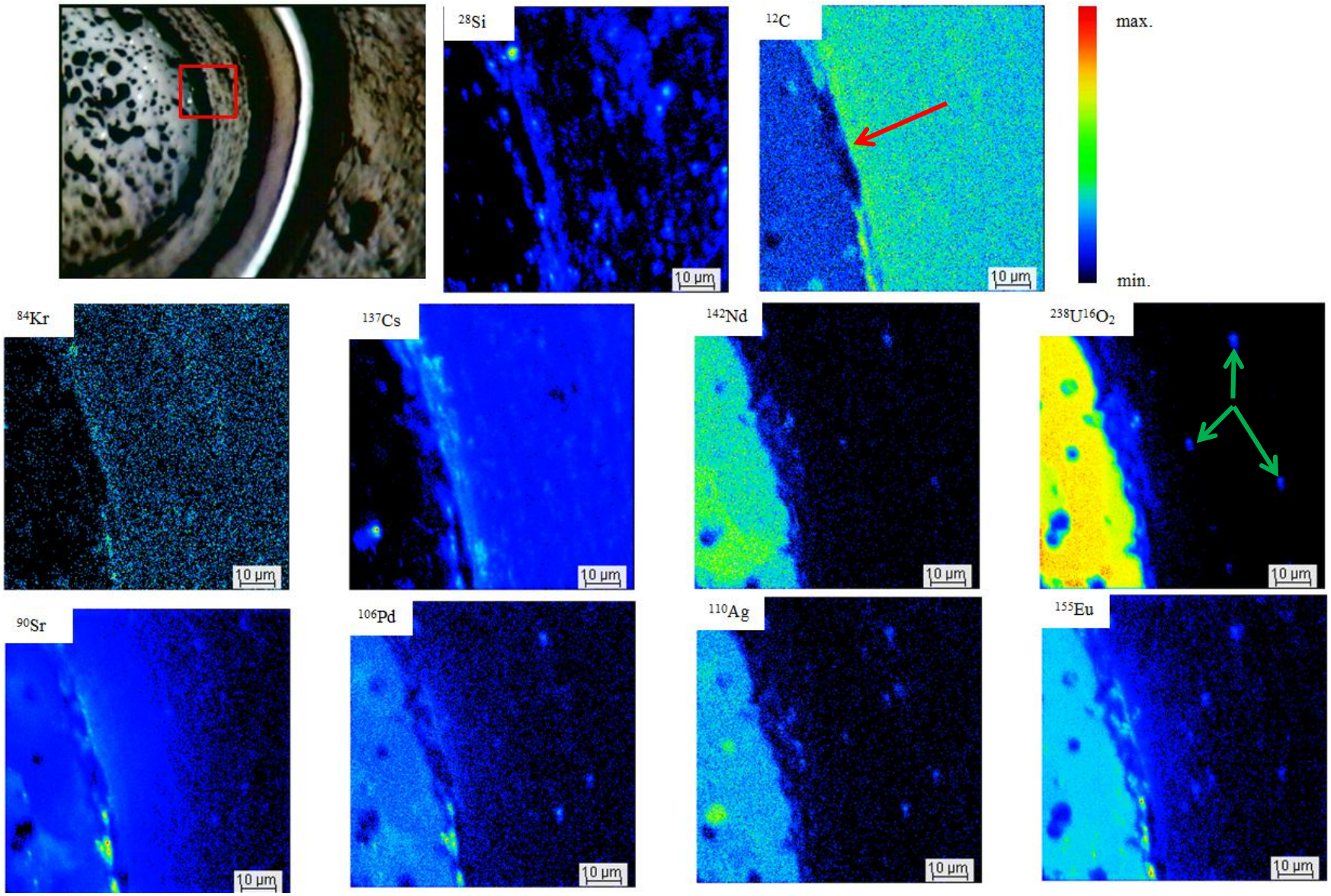

Fig 17: Optical image and ion maps showing the distribution of ^{28}Si, ^{12}C, ^{84}Kr, ^{137}Cs, ^{142}Nd, $^{238}U^{16}O^{2}$, ^{90}Sr, ^{106}Pd, ^{110}Ag and ^{155}Eu in the fuel porous PyC interface. The red square on the optical image shows the analysed area.

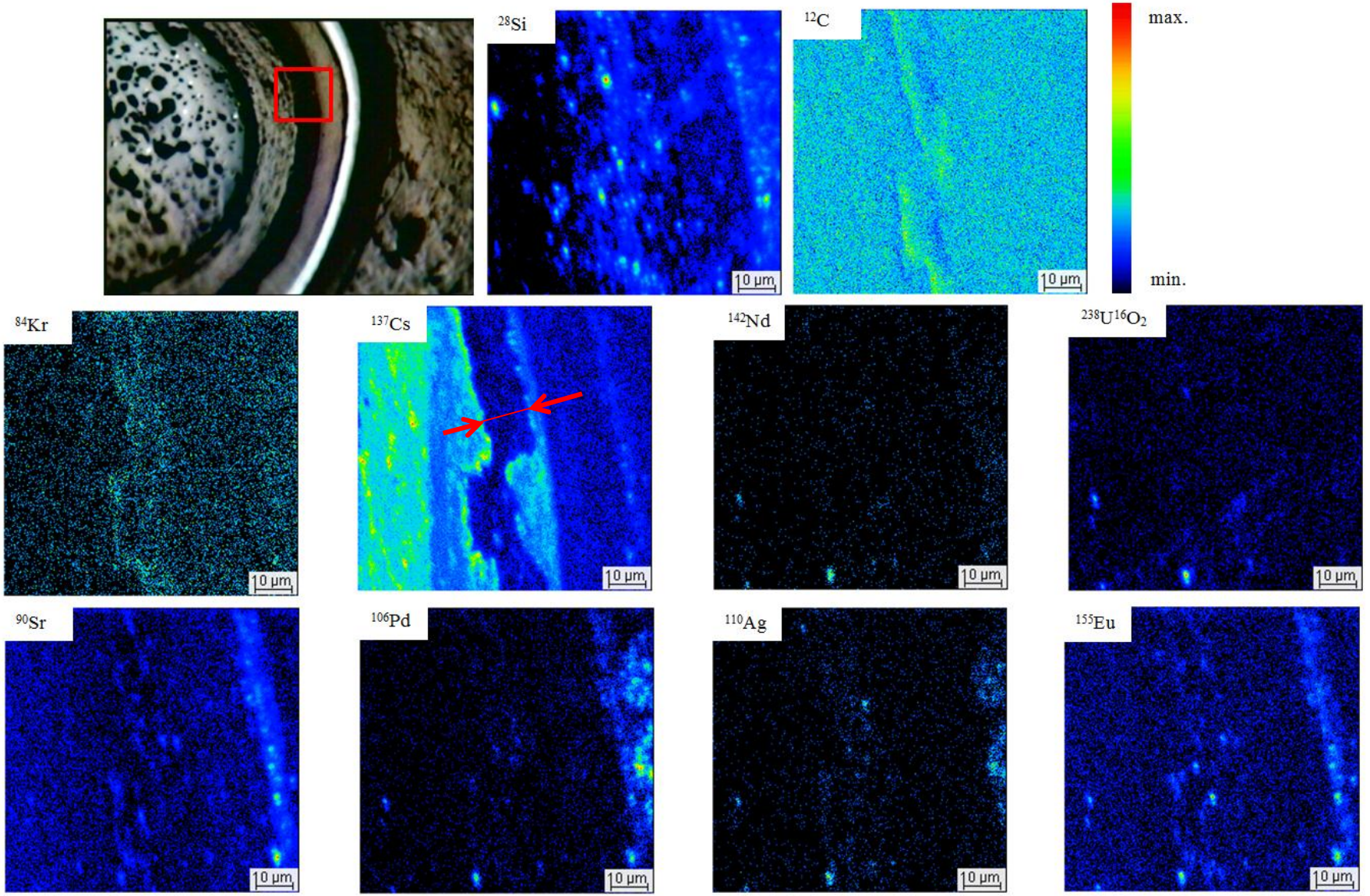

Fig 18: Optical image and ion maps showing the distribution of ^{28}Si, ^{12}C, ^{84}Kr, ^{137}Cs, ^{142}Nd, $^{238}U^{16}O^2$, ^{90}Sr, ^{106}Pd, ^{110}Ag and ^{155}Eu in the porous PyC dense PyC interface. The red square on the optical image shows the analysed area.

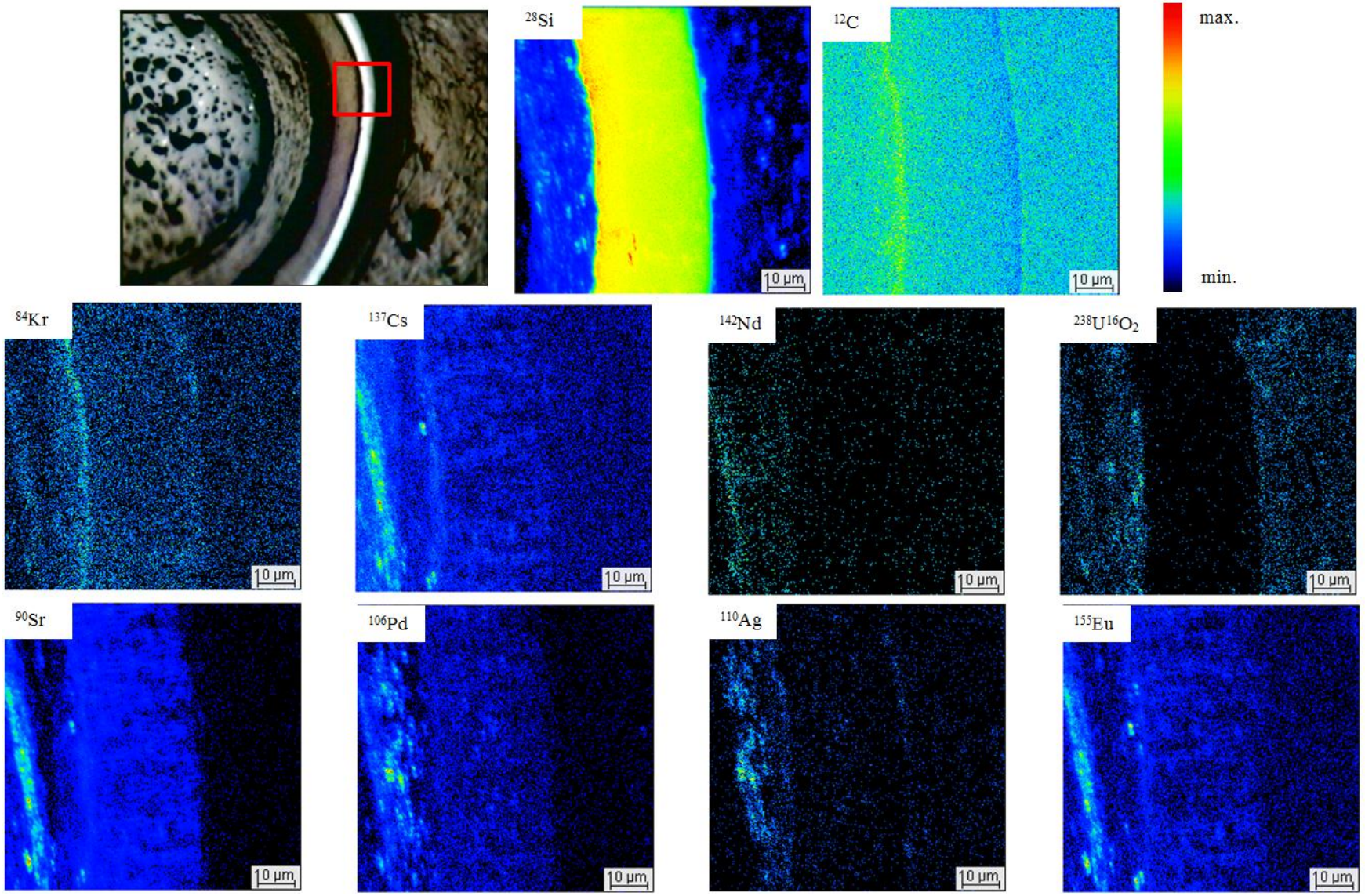

Fig 19: Optical image and ion maps showing the distribution of ^{28}Si, ^{12}C, ^{84}Kr, ^{137}Cs, ^{142}Nd, $^{238}U^{16}O^{2}$, ^{90}Sr, ^{106}Pd, ^{110}Ag and ^{155}Eu in the dense PyC/SiC interface. The red square on the optical image shows the analysed area.

9. Acoustic microscopy examination on sample 1076

Acoustic Microscopy is a powerful non-destructive tool able to reveal the material microstructure from the detection of the reflection conditions of a focused ultrasonic beam. With high frequency acoustic waves, variations of elastic properties can be locally investigated in solid materials from the analysis of the acoustic signature technique V(z) and the measurement of the Rayleigh velocity.

Due to a technical issue related to the LEMO connectors into the cell, the availability of the acoustic system was lately granted during the ARCHER timeframe.

Some acoustical images were lately performed on the sample 1076 with a 140 MHz detector. The change in material properties is translated by the use of a grey scale that generated the acoustical images depicted in fig. 20.

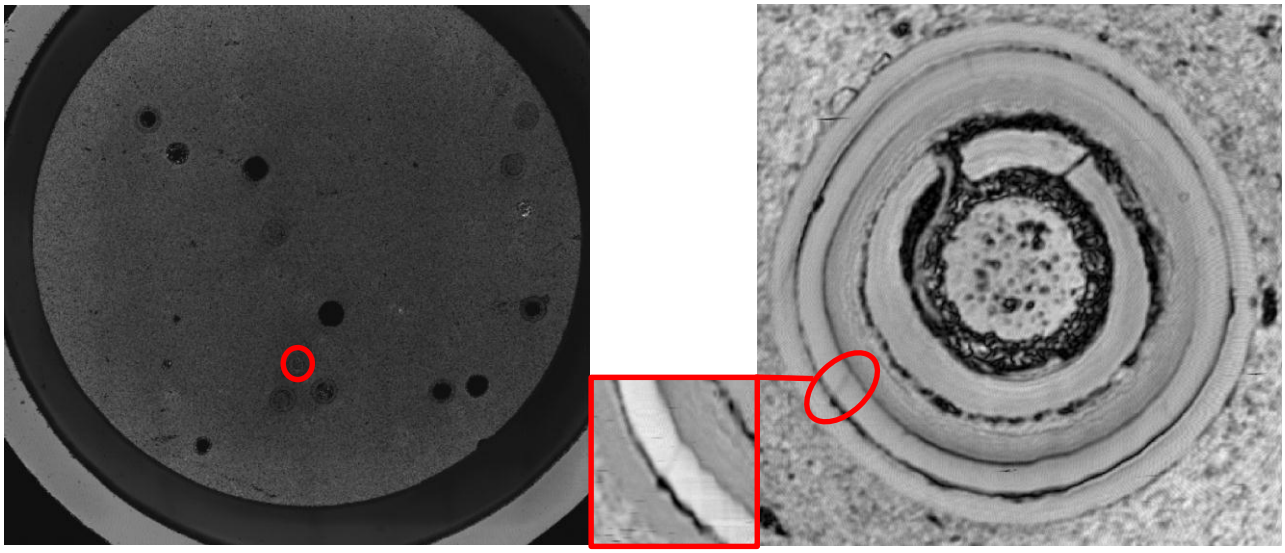

Fig 20: Acoustical image performed at 140 MHz (Left: global view of the sample, Right and middle: specific analysis of the particle in the red circle)

The black areas present in the Fig 20 (left) are representative of a void (i.e. it corresponds to particles where the fuel kernel dropped out during the polishing process). The porosity of the fuel as much as the delamination process and the porous PyC area also appeared in black in Fig. 20 (middle and right).
As expected, this acoustic technique promoted the detection of tiny cracks in the SiC layer that led to the high Cs release encountered during the KüFA test.

Some V(z) measurements have been performed on the fuel in order to determine a local Young modulus. Unfortunately the preliminary results at 82 MHz do not allow some accurate measurements. Some extra V(z) measurements performed at lower frequencies should allow more robust Young modulus estimation that may be linked with a Burn up determination.

10. Conclusion

In the framework of the ARCHER project, the HFR-EU1/3 pebble irradiated in the HFR-EU1 experiment was KüFA tested. The three samples originating from the carroting of the pebble were studied by different PIE means (mainly optical microscopy, SEM, SIMS and acoustic microscopy). Most of the coated particles that have been analyzed were found with radial cracking in the SiC layer. On the contrary to other PIE tests [6], some evidence for a significant deterioration in terms of mechanical or chemical attacks (due to CO, FPs) of the SiC layer due to the Küfa heating test up to 1800°C were detected. The relatively large failure fraction is due to the Küfa testing temperature that was maintained at a real 1800°C temperature plateau for 200 hours resulted in significant FP release (e.g. about 70% of the Cs was released at the end of the KüFA test). If a good adhesion was observed between the SiC layer and the outer pyrolytic carbon layer, some delamination

phenomena were observed both between the outer pyrolytic carbon layers and at the matrix interface. Unfortunately, the EDX being out of order during the SEM examinations, no information could be collected on the local composition of the material.
SIMS measurements led to the conclusion that Ag and Pd may have been present as a couple at the interface of the SiC. Although SIMS examinations do not offer full explanation up to this point about the failure mechanism of the SiC layer, some further studies on several coated particles and especially in the vicinity of the SiC cracks will be pursued.
Some acoustic microscopy measurements, delayed due late technical issues in the hot cells, were also performed and the acoustical images achieved led to the detection of tiny cracks in the SiC layer. All the expected PIE were mostly delayed due to the late delivery of the pebbles at JRC-ITU (i.e. about one year delay when dealing with the original PIE timetable). The remaining data will be merged in a synthetic document that will be made available to the ARCHER participants.

11. References

[1] M. Laurie, A.Marmier, M. A. Fütterer; “Results of the HFR-EU1 Fuel Irradiation of INET and AVR Pebbles in the HFR Petten”; Proceedings of HTR 2010; Paper 050; 2010

[2] D. Freis, Störfallsimulationen und Nachbestrahlungsuntersuchungen an kugelförmigen Brennelementen für Hochtemperaturreaktoren, PhD Thesis, 2010.D.

[3] HFR-EU1 depletion calculations - ARCHER Project Deliverable D32.31

[4] S. Brémier, R. Hasnaoui, S. Portier, O. Bildstein and C.T. Walker, Microchim. Acta 155 (2006) 113.

[5] Y. Ranebo, M. Eriksson, G. Tamborini, N. Niagolova, O. Bildstein and M. Betti, Microsc. Microanal. 13 (2007) 179.

[6] S. de Groot et al., 4th International Topical Meeting on High Temperature Reactor Technology, Washington (DC), USA, 2008, vol. 1, p. 307